ELSEVIER

Nuclear Instruments and Methods in Physics Research A 447 (2000) 151–159

NUCLEAR INSTRUMENTS & METHODS IN PHYSICS RESEARCH Section A

www.elsevier.nl/locate/nima

Cryogenic operation of silicon detectors

P. Collins[a,*], I.B.M. Barnett[b], P. Bartalini[c], W. Bell[d], P. Berglund[e], W. de Boer[f], S. Buontempo[g], K. Borer[h], T. Bowcock[i], J. Buytaert[a], L. Casagrande[j], V. Chabaud[a], P. Chochula[k], V. Cindro[l], C. Da Via[m], S. Devine[d], H. Dijkstra[a,1], B. Dezillie[n], Z. Dimcovski[o], O. Dormond[c], V. Eremin[p], A. Esposito[q,m], R. Frei[c], V. Granata[r], E. Grigoriev[f,o], F. Hauler[f], S. Heising[f], S. Janos[h], L. Jungermann[f], Z. Li[n], C. Lourenço[a], M. Mikuž[l], T.O. Niinikoski[a], V. O'Shea[d], V.G. Palmieri[a], S. Paul[m], C. Parkes[a], G. Ruggiero[g], T. Ruf[a], S. Saladino[a], L. Schmitt[m], K. Smith[d], I. Stavitski[s], E. Verbitskaya[p], F. Vitobello[r], M. Zavrtanik[l,t]

[a]*CERN, EP Division CH-1211, Geneva 23, Switzerland*
[b]*Institut für Kernphysik, Johannes Gutenberg-Universität Mainz, Johann-Joachim-Becher-Weg 45, D-55099 Mainz, Germany*
[c]*Institut de Physique des Hautes Energies, Batiment des Sciences Physiques, Université de Lausanne, CH-1015 Dorigny 20, Switzerland*
[d]*Department of Physics and Astronomy, University of Glasgow, Glasgow G12 8QQ, UK*
[e]*Helsinki University of Technology, Espoo, Finland*
[f]*IEKP, Universität Karlsruhe, Engesserstr. 7, 76128 Karlsruhe, Germany*
[g]*Universita' Frederico II di Napoli, Dipartimento di Fisica and INFN, via Cinthia 1, Monte Sant'Angelo, Napoli, Italy*
[h]*Laboratorium für Hocherergiephysik der Universität Bern, Sidlerstr.5,CH 3012 Bern, Switzerland*
[i]*Department of Physics, Oliver Lodge Laboratory, Liverpool, L69 7ZE, UK*
[j]*LIP, av. E. Garcia 14, P-1000 Lisbon, Portugal*
[k]*Comenius University, Mlynska dolina F1, SK 84215 Bratislava, Slovakia*
[l]*Jožef Stefan Institute and Department of Physics, University of Ljubljana, SI-1000 Ljubljana, Slovenia*
[m]*Physik Department E18, Technische Universität München, James Franck Strasse, D-85748 Garching, Germany*
[n]*Brookhaven National Lab, PO Box 5000, Upton, NY 11973-5000, USA*
[o]*University of Geneva, Department of Radiology, Geneva, Switzerland*
[p]*Ioffe Physico Technical Institute of Russian Academy of Sciences, 194021 St.-Petersburg, Russia*
[q]*Electrotechnical Laboratory,Electron Devices Division,1-1-4 Umezono, Tsukuba,305-8568 Ibaraki, Japan*
[r]*Istituto di Cibernetica del CNR, Via Toiano 6, 80072 Arco Felice, Italy*
[s]*Dipartimento di Fisica, Università di Padova and INFN, Via Marzolo 8, I-35131 Padova, Italy*
[t]*INFN and University of Florence, Florence, Italy*

Abstract

This paper reports on measurements at cryogenic temperatures of a silicon microstrip detector irradiated with 24 GeV protons to a fluence of 3.5×10^{14} p/cm^2 and of a p–n junction diode detector irradiated to a similar fluence. At temperatures below 130 K a recovery of charge collection efficiency and resolution is observed. Under reverse bias conditions this recovery degrades in time towards some saturated value. The recovery is interpreted qualitatively as

* Corresponding author.
[1] Also corresponding author.
E-mail address: paula.collins@cern.ch (P. Collins).

PII: S0168-9002(00)00183-2

changes in the effective space charge of the detector causing alterations in the depletion voltage.

PACS: 61.82.Fk

Keywords: Silicon detectors; Radiation damage; Position resolution

1. Introduction

This paper overviews some results from the RD39 collaboration on the cryogenic operation of irradiated silicon detectors, and the dramatic improvements in charge collection efficiency (CCE) which can be observed at low temperatures, a phenomenon known as the "Lazarus effect" [1]. This paper is devoted mainly to a discussion of the regime of irradiation fluences corresponding to 10^{14} n/cm^2 of 1 MeV neutrons, and the effects seen in situations of partial depletion. Results are presented from a test-beam, performed in collaboration with the DELPHI, LHCb and COMPASS experiments, which characterise the behaviour at cryogenic temperatures of a double-sided microstrip detector after irradiation with 24 GeV protons to a fluence of 3.5×10^{14} p/cm^2. In the first part of this paper we present a simple model which explains qualitatively the behaviour at cryogenic temperatures of irradiated silicon detectors, and predicts the consequences for a microstrip detector for the cluster shapes, or charge distribution on the strips, on both the ohmic (n) and junction (p) sides of the detector. We then present the results and show the agreement with the model. The behaviour is compared qualitatively to the behaviour of a p–n junction diode detector irradiated to similar fluence.

1.1. Radiation damage and strip detectors

The voltage needed to fully deplete a silicon detector, or "full depletion voltage" V_{fd} is given by

$$V_{\mathrm{fd}} = \frac{q}{2\varepsilon_0 \varepsilon_{\mathrm{s}}} \times D^2 \times |N_{\mathrm{eff}}| \qquad (1)$$

where q is the electron charge, ε_{s} the permittivity of silicon, ε_0 the permittivity of free space, D the detector thickness and N_{eff} the effective doping density, which is assumed here to be uniform. For a high-resistivity non-irradiated n-type silicon detector such as is generally used for silicon strip devices the value of N_{eff} is positive and between 10^{12} and $10^{13}\mathrm{cm}^{-3}$. During irradiation the introduction of deep levels modifies the value of N_{eff} for a detector under bias, making it progressively more negative. Up to a fluence equivalent of around 10^{13} n/cm^2 of 1 MeV neutrons the full depletion voltage falls. When $N_{\mathrm{eff}} \simeq 0$ the detector passes through a so-called inversion point, where the junction moves from the p-side to the n-side, after which the full depletion voltage steadily rises as N_{eff} becomes more negative. The fluence levels discussed in this paper of around 10^{14} n/cm^2 are roughly equivalent to 10 years of operation at the first silicon barrel of the ATLAS experiment at the LHC, or 1 year of operation of the vertex detector of the LHCb experiment. At these fluences the full depletion voltages are expected to be between about 150 and 350 V [2,3], rising by a possible further 100–200 V after room temperature reverse annealing effects [2]. The range of values comes from strong dependences on the silicon producer, the uncertainties in extrapolating from diode measurements to strip detectors, and the uncertainties from the frequency at which the classical C–V measurements are made. In practical terms, it may be that the full depletion voltage is higher than that which can be applied. Possible reasons could be electrical breakdown, thermal runaway, or a higher than expected radiation environment can cause the full depletion voltage to exceed the system design. In such a case, the detector must be operated underdepleted.

For a strip detector the consequences of under-depleted operation are loss of efficiency and loss of resolution, particularly on the p-side. This is illustrated in Fig. 1 which shows an irradiated partially depleted detector. The electric field gradient

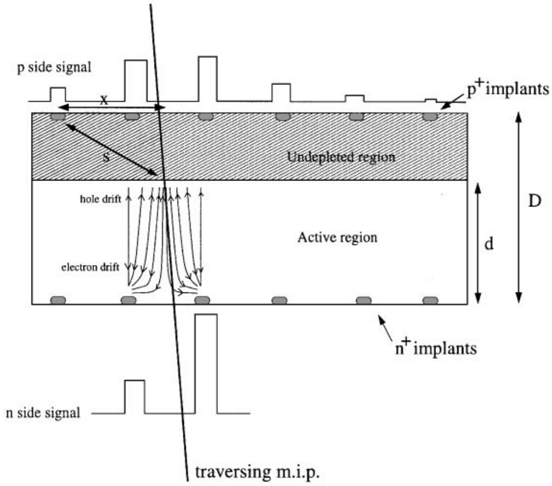

Fig. 1. Sketch illustrating the accumulated charge resulting from the passage of a minimum ionising particle (m.i.p.) for a partially depleted double-sided detector. The total charge collected on the n- and p-side is the same, and the CCE is equal to d^2/D^2, if all the charge loss is assumed to be due to underdepletion.

extends from the n-side of the detector through the active region, dropping to zero at the edge of the non-depleted layer. The efficiency in this case drops due to the fact that only the electrons and holes generated in the active layer contribute to the signal. In addition, the non-depleted layer for a heavily irradiated detector acts as an insulator for the current pulse, and the total charge seen on the detector surface is proportional to the ratio of the drift distance (or active layer) to the detector thickness [4]. The total charge seen is therefore proportional to $(d/D)^2$, where d is the thickness of the active layer and D the detector thickness, or to the depletion voltage V, assuming uniform space charge. This relation has been demonstrated experimentally, for instance in Ref. [5].

On the n-side the electrons drift towards the strips in the same way as for a non-irradiated detector, and the accuracy of the track position measurement is not reduced. On the p-side, the strips are separated from the active region by the insulating non-depleted layer and an image charge is seen. We postulate in this paper a simple model that the image charge seen on a strip is inversely proportional to $s^2 = x^2 + (D - d)^2$, where s is the distance between the strip and the impact point of the track on the non-depleted layer (see Fig. 1). This has the effect that the charge is spread over many strips, particularly if the pitch on the p-side is fine with respect to the width of the non-depleted region. In a practical experiment the precise measurement of the cluster shape will be limited by noise and the resolution will be degraded. In addition, the efficiency on the p-side can be further affected, if the signals on individual strips fall below the signal-to-noise threshold. Note that if there is a drop in CCE due principally to under-depletion, then both the shape and the absolute magnitude of signal on each strip are controlled by one parameter, the depletion depth. The depletion depth which is inferred from the cluster shape on the p-side should agree with the depletion depth measured on the n-side via $\mathrm{CCE} = d^2/D^2$, and this is a powerful cross check. Note that due to this effect the n-side signal is the most reliable way to compare data from strip detectors with data from diode detectors.

1.2. Cryogenic operation

There are three principal considerations why cryogenic operation, which in this paper is to be understood as temperatures below $\simeq 130$ K, is predicted to be advantageous.

- At low temperatures one can eliminate the large leakage current which is generated in irradiated detectors and which can swamp the signals with noise and generate heat in the detectors. The expected reduction of leakage current is about a factor of 2 for each 5 K drop [6], and for strip detectors modest cooling is sufficient.
- For irradiated detectors there can be a loss of signal due to the fact that the signal charge is trapped in the energy levels, or traps, which develop after irradiation. The emission time of the traps τ_e depends strongly on the temperature:

$$\tau_e \propto \exp\frac{\Delta E}{kT} \tag{2}$$

where ΔE is the trap level energy relative to the conduction or valence band, T is the temperature and k the Boltzmann constant. At very low temperatures τ_e becomes very long compared to the charge collection time, and the traps can "freeze-out", i.e. they are filled by some earlier charge passage, for instance from the leakage current, and do not trap the signal charge.

- A further consequence of the "freeze out" of the traps is that the filling of the traps modifies the overall space charge and hence the full depletion voltage. This is illustrated in Fig. 2. Even if the detector has developed a large and negative N_{eff} after irradiation, then by hole trapping N_{eff} can be made more positive and hence the full depletion voltage reduced. The mechanism for the trap filling could be a combination of cryogenic operation to freeze out the traps, plus a deliberately introduced hole current, and this approach has been pursued in Ref. [7]. The effect of the modification of the space charge at low temperatures is the most important effect discussed in this paper.

2. Experimental detectors

The DELPHI module used was a half-module of the 1994 DELPHI [8,9] vertex detector, described in detail in [10]. The module consisted of two double-sided AC coupled $5.4 \times 3.2\ \mathrm{cm}^2$ silicon microstrip sensors, with the p-side reading out the coordinate along the length of the module, and the n-side reading out the orthogonal coordinate, with the signal being routed to the electronics via a double-metal strip arrangement. The electronic shaping time used during this experiment was 8 μs. The module was irradiated towards the tip to avoid damaging the radiation-soft electronics [11], hence the radiation was inhomogeneous and situated mainly on the sensor furthest away from the hybrid. On this sensor the strip pitch on the p (n)-side was 25 μm (42 μm) and the readout pitch was 50 μm (42 μm). The sensor was 310 μm thick. The unbiased detector was irradiated at room temperature with 3.5×10^{14} 24 GeV protons/cm^2 in the CERN-PS. Before the test-beam it was annealed for about 9 days at a temperatures between 25°C and 30°C. Soon after the irradiation it drew 1 mA at 65 V at room temperature. The current was re-measured after 8 months of storage at room temperature and found to be 20 μA at 250 K with a bias voltage of 90 V.

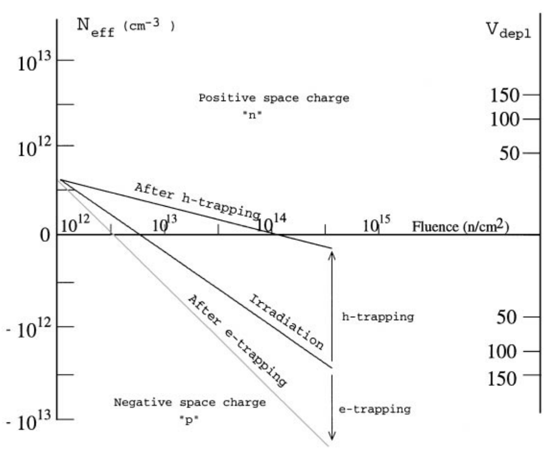

Fig. 2. Sketch illustrating the behaviour of the space charge during irradiation, and how it might be modified at cryogenic temperatures by hole or electron trapping.

The diode detector sample described in this paper was a 350 μm thick DC coupled-implanted device processed at BNL.[2] The sensitive area is $5 \times 5\ \mathrm{mm}^2$, surrounded by a guard ring. The diode was irradiated uniformly with neutrons at the TRIGA reactor in Ljubljana, Slovenia to an equivalent fluence of 1×10^{14} n/cm^2 of 1 MeV neutrons, and heated to achieve an annealing factor corresponding to about 1 year of room temperature storage. Using a conversion factor of 0.51 for 24 GeV protons [12,13] this fluence is about half of the fluence received by the strip detector. Taking the annealing into account the samples are roughly comparable.

3. Experimental setups

The irradiated microstrip detector was tested in a 100 GeV/c muon test-beam. An Oxford Variox BL beam cryostat consisting of an evacuated insert in a liquid He reservoir with a shield cooled by

[2] Brookhaven National Lab, PO Box 5000, Upton, NY 11973-5000, USA.

liquid N_2 was used. The detector was mounted together with a double-sided reference detector inside a section protruding below the cryostat and equipped with thin aluminised mylar windows. The temperature was monitored with PT100 resistors placed on the hybrids and on the chamber walls. The geometry is illustrated in Fig. 3. The test beam illuminated a $\sim 3 \times 3$ cm^2 area on the surface of the sensor, covering the most irradiated region. Using the reference module and the beam telescope extrapolation [14] the impact point of the track on the irradiated detector was known with a precision of about 5 μm (13 μm) for the p-side (n-side) coordinate. A total of about 300,000 tracks were collected. About two-thirds of the data were collected in a set of 15 min runs at hybrid temperatures between 117 and 150 K and bias voltages between 10 and 90 V. The remainder were collected in a run lasting 150 min at a hybrid temperature of 136 K and a bias voltage of 90 V. The temperature on the detector was about 4° lower than that on the hybrid.

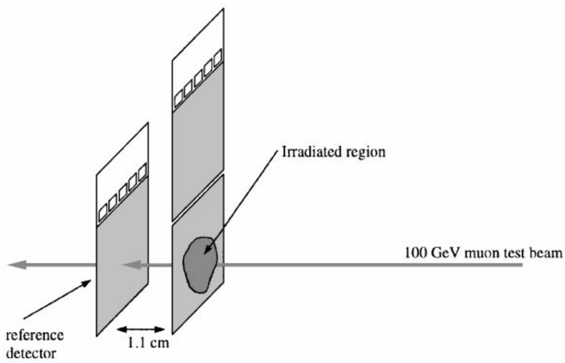

Fig. 3. Sketch of the test beam setup.

The irradiated diode was tested using a ^{90}Srβ source inside a vacuum-tight insert within a liquid nitrogen Dewar vessel [15]. A trigger diode was mounted behind the irradiated diode. By means of slow cooling the tests were performed at temperatures between 77 and 180 K. At higher temperatures the leakage current was too high to make measurements.

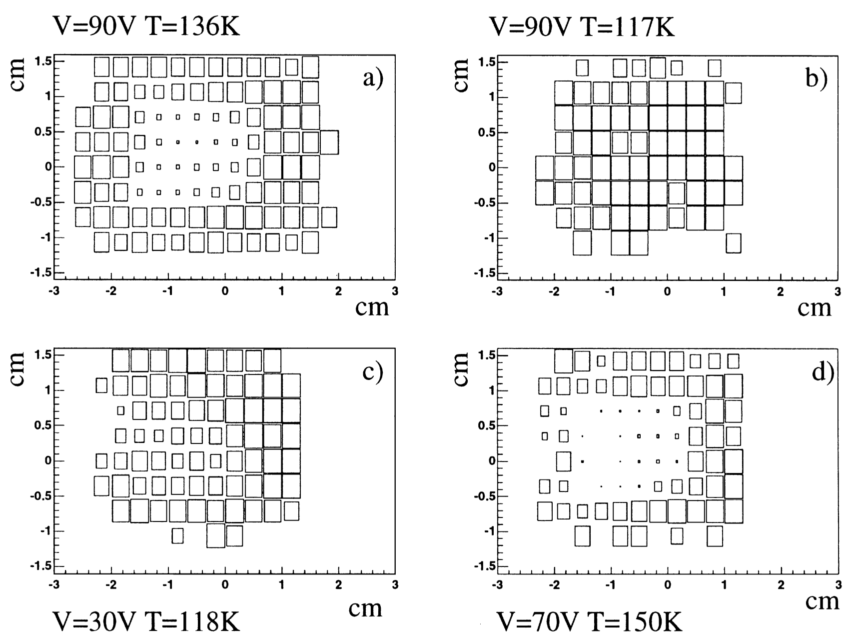

Fig. 4. Efficiency measured in different runs on the p-side of the detector using a cluster search algorithm. The size of the square indicates the efficiency at that point on the detector surface, with a full square indicating 100% efficiency. A minimum of 10 traversing tracks were required to give an entry in any bin, and the $\sim 3 \times 3$ cm^2 extent of the test beam can be seen. Where there is no entry it is due to insufficient statistics, apart from the enclosed area in figure (d) where there are four points of zero efficiency. The run illustrated in figure (a) lasted for 150 min, and the other runs lasted for about 15 min, hence the better statistics in this plot.

4. Efficiency and CCE results

The efficiency was measured by applying a cluster search algorithm to the irradiated sensor. A good cluster was required to have at least one channel with a signal-to-noise ratio (S/N) greater than four, with both neighbours having a smaller S/N. The noise of the DELPHI module was approximately 1250 (1350) electrons per channel on the p-side (n-side), hence for a non-irradiated module this algorithm gives an efficiency, defined as the chance that a cluster is reconstructed at the position where the track passed through, close to 100%. The results for the p-side efficiency on the irradiated detector are shown in Fig. 4. At a bias voltage of 90 V and a temperature of 136 K the behaviour is close to what is expected, showing a drop in efficiency in the central irradiated region due to the fact that the bias voltage is insufficient to deplete the detector in this region.

At a temperature of around 117 K there is a dramatic change, and the irradiated part of the detector becomes efficient. Even with a bias voltage of 30 V there is some recovery seen in this region at the lower temperature. Conversely, going to the higher temperature, even with a high-bias voltage, the performance is much worse.

On the n-side a similar behaviour is seen. Here it is more convenient to present the results in terms of charge collection efficiency, or CCE, as due to the fact that the clusters are not spread as the changes in efficiency are not so dramatic as for the p-side. The CCE is measured by extrapolating the track to the module and summing the charge measured in four strips on either side of the impact point of the track. The resulting histogram is fitted with a Landau smeared with a function to approximate the noise of the DELPHI module. The CCE is given by the most probable value of the Landau fit divided by the calibration value, C_0, which is the charge which is expected to be deposited by a minimum ionising particle (m.i.p) in a fully depleted non-irradiated detector. C_0 is measured independently for each of the 10 chips using regions far away from the irradiated regions. The CCE measured on the n-side is shown in Fig. 5 for two runs corresponding to those illustrated in Fig. 4. At warmer temperatures the CCE corresponds to that expected for

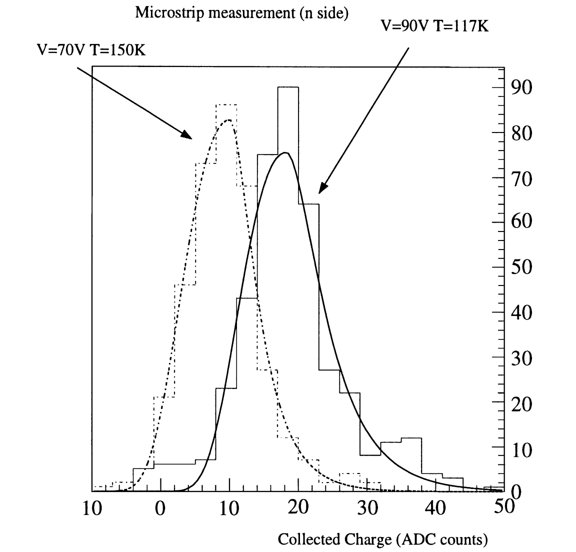

Fig. 5. CCE measured on the n-side of the detector in the central, most irradiated region, for two runs corresponding to Figs. 4 (b) (solid line) and 4 (d) (dashed line). The most probable peak of the fitted Landau corresponds to CCE measurements of 95% and 50%, respectively.

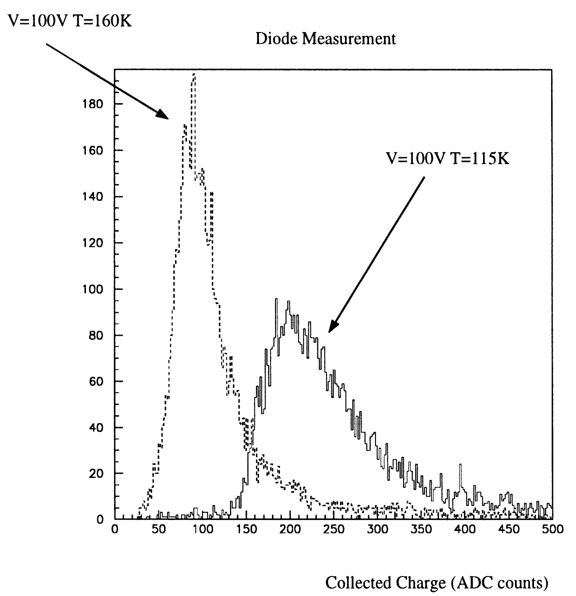

Fig. 6. Collected charge in ADC counts measured on the diode at two different temperatures and at modest bias voltage. The curves correspond to CCE values of approximately 35% and 80% at 160 and 115 K, respectively.

a not-fully-depleted detector, while at the lower temperatures the voltage seems to be sufficient to fully deplete and collect the full charge.

The CCE on the diode was measured by exposing the p-side to electrons and selecting minimum ionising particles using the trigger diode. The signal was read out from the n-side of the detector via a decoupling capacitor using a GaAs FET. The charge signal was shaped with a time of 1 μs and recorded in a multi-channel analyser. The calibration was obtained by comparing the signal to that obtained from a non-irradiated diode of similar thickness operated above full-depletion voltage. The behaviour of the diode at different temperatures is illustrated in Fig. 6. A depletion voltage of 100 V is used, at which the diode is expected to be underdepleted. However, at the lower temperature a significant recovery in charge collection is seen.

5. Cluster shape and resolution results

For each run the cluster shape was measured on the n and p-sides, for the inner, or most irradiated region, the outer, or least irradiated region, and the area lying between. In order to compare with the p-side cluster model the CCE on the n-side was used to estimate the depletion depth, and from this the shape and height of the cluster were predicted. The results are illustrated in Fig. 7, which shows the charge collected on the $\pm$ 1st, $\pm$ 2nd, $\pm$ 3rd and $\pm$ 4th strips, normalised to C_0, on either side of the

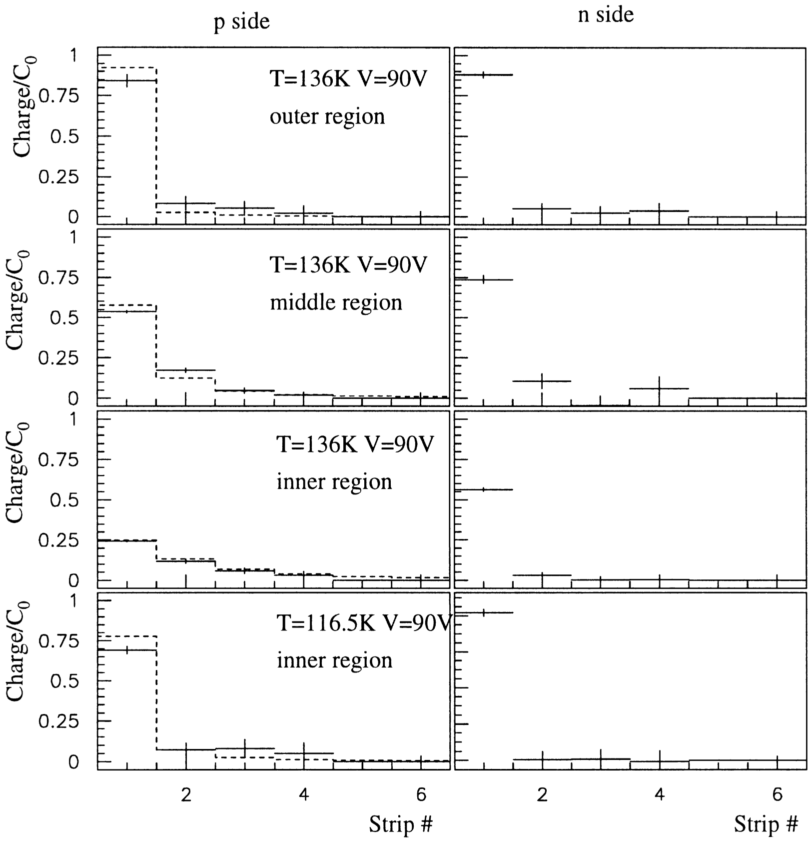

Fig. 7. Cluster shapes for the data (error bars) on the p-side and n-side, and the p-side model (dashed line). The histograms show the charge accumulated on the $\pm$ 1st, $\pm$ 2nd, $\pm$ 3rd, etc. strips to either side of the track impact point, divided by the total charge which a m.i.p is expected to deposit in a non-irradiated fully depleted detector.

track impact point. For the data the charge was not measured for strips further away as at this point the noise dominates. The three areas are shown for the run at 90 V bias and 136 K, and the most irradiated area is shown for the run which shows the most dramatic charge recovery. On the n-side it can be seen that even when there is charge loss the cluster remains focused. On the p-side there is good agreement with the model, which predicts that when there is loss of charge due to non-depletion this goes hand-in-hand with cluster spread. For the very cold run charge becomes focused again, in parallel with the CCE recovery. This behaviour indicates that the "Lazarus effect" is linked to changes in space charge and depletion depth.

The resolutions measured correspond to what is expected from the cluster shapes. On the n-side the resolution was measured to be close to 12 μm at all CCE values. This resolution is close to the 9 μm expected for a detector with 42 μm strip pitch. On the p-side, the resolution was found to be 11 μm for CCE values of close to 100%. However, the resolution on this side degraded rapidly with a fall in CCE, exceeding 100 μm at a CCE of 20%.

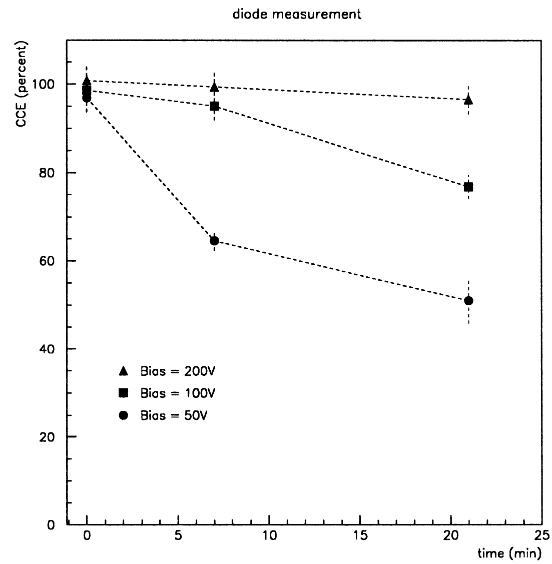

Fig. 8. CCE as a function of time measured on the diode detector for three different bias voltages at a temperature of 77 K.

6. Time dependence

Most of the data from the microstrip test beam were accumulated in relatively short runs of about 15 min. It was however observed that when there is a CCE recovery, there is also a decay in time of both CCE and resolution. After periods of between 5 and 20 min, the CCE approached values close to the values measured at higher temperatures. This effect was studied in detail in the measurements on diode detectors. A procedure was established to let the unbiased diode stabilise for 15 min, after which the voltage was applied and the measurements started. In Fig. 8 the CCE is shown as a function of voltage at different times after the raising of the bias voltage. At the lower voltages there is a clear decay in time. For higher voltage however the detector appears to be fully biased at all times.

Time-dependent effects after changing the bias voltage have been previously observed and historically were given the name of polarisation effects [16]. The time-dependent effects in this case may be understood as a result of the initial setting of the space charge after the application of the bias voltage moving gradually to a new equilibrium as traps empty or fill, which may be on very large time scales due to the long-emission times in the cold. Work is in progress to try to establish a quantitative explanation, for instance Ref. [17].

7. Conclusions and prospects

A module from the DELPHI experiment made with double-sided microstrip sensors has been irradiated and tested at cryogenic temperatures. At temperatures below $\simeq 130$ K and modest bias voltage there is a striking recovery of the CCE in the irradiated region, an effect known as the Lazarus effect. In parallel with the recovery in CCE the clusters become focused and there is a recovery in resolution. These effects however decay in time.

The observed effects may be interpreted as changes in the space charge density. After irradiation the detector is operating in a regime where it is partially depleted at 90 V. Changes in the space charge which lead to the detector becoming fully depleted at the same bias voltage lead to dramatic recoveries in the CCE and resolution. At cryogenic temperatures the "freeze out" of the traps makes this space charge modification possible. The time-dependent effects are interpreted as imbalances between trap filling rate, which is dependent on quantities such as leakage current, and trap emission rate, dependent on temperature. It may well prove possible to control the "Lazarus effect" and eliminate the decay in time, and studies are underway in this direction, for instance Ref. [7].

Acknowledgements

The work described in this paper resulted from a joint effort among people from the RD39 collaboration and the DELPHI, COMPASS and LHCb experiments. We thank the IPHE-Lausanne, the LHEP-Bern and the CERN-EP Microelectronics workshops for technical support. We thank A. Hauska for participating in the setup preparation and S. Gerassimov for helpful discussions concerning the reference telescope. We are grateful to C. Buttar, P. Riedler and J. Wüstenfeld for help with the ATLAS CERN-PS irradiation facility. We thank L. Beattie, P. Riedler and S. Watts for illuminating discussions. K. Pretzl and P. Sonderegger are warmly acknowledged for their continuous support.

This research was supported by the Schweizer Nationalfonds zur Förderung der wissenschaftlichen Forschung (FORCE) and by the Stiftung zur Förderung der wissenschaftlichen Forschung an der Universität Bern. One of the authors (L.C.) acknowledges financial support from the EC (TMR programme) under contract number ERBFMBICT961204. One of the authors (S.D.) acknowledges financial support from the Particle Physics and Astronomy Research Council and the Rutherford Appleton Laboratory CASE award. The work of two of the authors (B.D. and Z.L.) was supported by the US Department of Energy, Contract Number DE-AC02-98CH10886.

References

[1] V.G. Palmieri et al., Nucl. Instr. and Meth. A 413 (1998) 475.
[2] D. Morgan et al., Nucl. Instr. and Meth. A 426 (1999) 336.
[3] A. Ruzin, Nucl. Instr. and Meth. A 447 (2000) 116, these proceedings.
[4] G. Cavalleri et al., Nucl. Instr. and Meth. 92 (1971) 137.
[5] L. Beattie et al., Nucl. Instr. and Meth. A 412 (1998) 238.
[6] D. Morgan et al., Nucl. Instr. and Meth. A 326 (1993) 373.
[7] Z. Li et al., Improved neutron radiation hardness for Si detectors: application of low resistivity starting material and/or manipulation of N_{eff} by selective filling of radiation-induced traps at low temperatures, Presented at NSS 1998, Toronto, Canada.
[8] DELPHI Coll., P. Aarnio et al., Nucl. Instr. and Meth. A 303 (1991) 233.
[9] DELPHI Coll., P. Abreu et al., Nucl. Instr and Meth A 378 (1996) 57.
[10] V. Chabaud et al., Nucl. Instr. and Meth. A 368 (1996) 314.
[11] P. Seller et al., Nucl. Instr. and Meth. A 315 (1992) 393.
[12] G. Lindstrom et al., Nucl. Instr. and Meth. A 426 (1999) 1.
[13] M. Moll et al., Nucl. Instr. and Meth. A 426 (1999) 87.
[14] W. Bruckner et al., Nucl. Instr. and Meth. A 348 (1994) 444.
[15] V.G. Palmieri et al., Nucl. Instr. and Meth. 417 (1998) 111.
[16] V. Eremin et al., Sov. Phys. Tech. Semicond. 8 (6) (1974) 751.
[17] V. Eremin, N. Strokou, E. Verbitskaya, Z. Li, Nucl. Instr. and Meth. 372 (1996) 388.